Electric Power Systems Research 154 (2018) 13–22

Contents lists available at ScienceDirect

Electric Power Systems Research

journal homepage: www.elsevier.com/locate/epsr

# Determining optimal virtual inertia and frequency control parameters to preserve the frequency stability in islanded microgrids with high penetration of renewables

Masoud Hajiakbari Fini, Mohamad Esmail Hamedani Golshan*

*Department of Electrical and Computer Engineering, Isfahan University of Technology, Isfahan, Iran*

ARTICLE INFO

*Article history:*
Received 25 January 2017
Received in revised form 8 July 2017
Accepted 8 August 2017

*Keywords:*
Frequency stability
Low inertia microgrids
Many-objective optimization
Renewable energy resources
Virtual inertia

ABSTRACT

Preserving the frequency stability of low inertia microgrids (MGs) with high penetration of renewables is a serious challenge. To rise to this challenge, the inertia constant of MGs would be virtually increased using energy storages. However, it is important to determine the suitable value of inertia constant for these systems such that the frequency stability is preserved with a lower cost. Frequency droop coefficient of distributed energy resources (DERs) and load frequency controllers' parameters would also affect the frequency response of MGs. Hence, in this paper, inertia constant is tuned together with frequency droop coefficient of DERs and load frequency controllers' parameters. Determining these parameters is modeled as a multi-objective optimization problem and, because the number of objectives is higher than three, the problem is solved by a many-objective optimization algorithm. Comparative simulation studies have been done on an MG with different types of DERs to prove that using the proposed strategy for tuning the MG parameters not only the frequency deviation is highly decreased but also the amount of load shedding is considerably diminished. This would increase the customers' satisfaction. Moreover, considering the inertia constant as a minimization objective, frequency stability would be preserved with a lower cost.


## 1. Introduction

Due to the environmental concerns, there is an increasing interest in using renewable energy sources (RESs) for power generation. MGs would provide a suitable infrastructure for integrating RESs to the grid at distribution level. MGs can operate in grid-connected or islanded mode. However, in islanded mode, they would encounter challenges in frequency and voltage control. These problems would be exacerbated in MGs with a high share of power-electronically interfaced DERs; due to the low inertia of the grid. In fact, in low inertia MGs, power imbalances result in rapid changes in frequency that might endanger the stability of the system [1].

To address these stability concerns, some methods have been proposed to increase the inertia of MGs. In Refs. [2,3], using synchronous condensers have been proposed for this purpose. In addition to contributing to the inertia of the gird, synchronous condensers would participate in reactive power control. Inverter-based DERs would also emulate the inertial response of synchronous generators by injecting a power proportional to frequency derivative to the grid. In Ref. [4], a control method has been proposed for converters to emulate the behavior of synchronous generators. Virtual inertia has been implemented in Ref. [5] to increase the contribution of distributed generators to oscillation damping. To emulate the inertial behavior of synchronous generators, inverter-based DERs require a temporary source of energy similar to the kinetic energy of the rotor of synchronous generators. In Ref. [6], the energy stored in the rotor of doubly fed induction generator (DFIG) based wind turbines and also the ultracapacitor (UC) installed at the dc-link of converters are used as energy sources for inertia emulation. In Ref. [7], HVDC transmission line is controlled to contribute to the inertia of the grid. HVDC links would transfer the inertial power generated by wind farms to the main grid, transfer inertial power from one area of power system to another area or use the energy stored in the DC link to emulate the inertial response. UC is proposed in Ref. [8] to emulate the inertial response of synchronous generators in an isolated power system. Although some studies have been carried out on contribution of inverter-based DERs to the inertia of MGs, to the best of authors' knowledge, a systematic method for determining the proper value for inertia constant in islanded MGs has not yet been proposed.

* Corresponding author.
*E-mail addresses:* m.hajiakbari@ec.iut.ac.ir (M. Hajiakbari Fini), hgolshan@cc.iut.ac.ir (M.E. Hamedani Golshan).

http://dx.doi.org/10.1016/j.epsr.2017.08.007
0378-7796/

**Nomenclature**

| | |
|---|---|
| $R$ | Frequency droop coefficient of energy resources |
| $H$ | Inertia constant of the grid |
| $H_{vir}$ | Virtual inertia |
| $H_{eq}$ | The equivalent inertia constant of synchronous generators |
| $P_{ref-old}$ | Reference power of energy resources without inertia emulation |
| $P_{ref-new}$ | Reference power of energy resources with inertia emulation |
| $f$ | Operation frequency of the grid |
| $E$ | The energy required by UC for inertia emulation |
| $P_{inertia}$ | Inertial power |
| $f_{init}$ | Frequency before the disturbance |
| $f_{crit}$ | Critical frequency |
| $t_{crit}$ | The time it takes the frequency to reach the critical frequency |
| $E_{avail}$ | The energy available from UC |
| $C$ | Capacitance of UC |
| $V_{init}$ | Initial voltage of UC |
| $V_{min}$ | Minimum permissible voltage of UC |
| $P_{base}$ | Base power of the grid |
| $V_n$ | Nominal voltage of UC |
| $P_n$ | Nominal power of UC |
| $f_{nadir}$ | Frequency undershoot |
| $f_{max}$ | Frequency overshoot |
| $t_{st}$ | Settling time of frequency |
| $Obj_i$ | The $i$th objective function |
| $t$ | Time |
| $Q_{L0}$ | Initial reactive power of load |
| $Q_L$ | Current values of the load's reactive power |
| $b$ | Coefficient of load reactive power dependency on voltage |
| $f_n$ | Nominal frequency |
| $t_{sim}$ | Simulation time |
| $\Delta f(t)$ | Deviation of the frequency from the nominal value |
| $f_{min}$ | Minimum desirable frequency |
| $x$ | Vector of decision variables |
| $n$ | The number of DERs that participate in frequency control |
| $x^{up}$ | The upper limit vector for the decision variables |
| $x^{low}$ | The lower limit vector for the decision variables |
| $Obj_{li}$ | The $i$th objective of the $l$th Pareto optimal solution |
| $m$ | The number of objectives |
| $Ideal\_Obj$ | Ideal objective vector |
| $Ideal\_Obj_i$ | The $i$th element of the ideal objective vector |
| $d^l$ | Sum of the normalized objectives of the $l$th Pareto solution |
| $T_g$ | Governor time constant |
| $T_t$ | Turbine time constant |
| $T_{BESS}$ | BESS time constant |
| $T_{UC}$ | UC time constant |
| $\dot{P}_{BESS}$ | BESS ramp rate |
| $\dot{P}_{DEG}$ | DEG ramp rate |
| $P_{L0}$ | Initial active power of load |
| $V_0$ | Initial voltage of load |
| $V$ | Voltage of the load bus |
| $P_L$ | Current values of the load active power |
| $a$ | Coefficient of load active power dependency on voltage |
| $K_{pf}$ | Coefficient of load active power dependency on frequency |
| $K_{qf}$ | Coefficient of load reactive power dependency on frequency |

In addition to inertia constant, load frequency controllers and frequency droop coefficient of power sources would affect the frequency response of the grid. Fine-tuning the load frequency controllers would reduce the maximum frequency deviation and also bring back the frequency to the nominal value faster. Different methods have been proposed for load frequency control (LFC) in power systems. In Ref. [9] the performance of model predictive controller for LFC in Nordic power system was investigated. Many researchers have focused on tuning the traditional proportional integral (PI)/proportional integral derivative (PID) controllers using evolutionary algorithms. In Ref. [10] bacterial foraging optimization algorithm has been implemented to tune the load frequency controllers of an MG with generation rate constraint (GRC). In Ref. [11] a hierarchical approach based on fuzzy logic has been proposed to improve the quality of frequency control. Electrical vehicles have been implemented in Ref. [12] for frequency control. In Ref. [13], fractional order PID controllers have been proposed for LFC in a multi-area power system. An adaptive set-point modulation technique has been implemented in Ref. [14] to enhance the performance of PI load frequency controllers. To improve the performance of frequency controllers in a three-area thermal power system, in Ref. [15] governors' frequency droop coefficient ($R$) have been optimized together with the load frequency controllers' parameters.

Since the grid inertia constant ($H$), frequency droop coefficient of DERs and parameters of load frequency controllers all affect the frequency response of MGs, in this paper, tuning these parameters has been suggested to improve the frequency stability of MGs. Based on different criteria that should be met to have a proper frequency response in MGs, a systematic method is proposed for tuning all the parameters, including $R$, $H$ and the controllers parameters, simultaneously. The main goal of tuning these parameters is to improve the frequency stability of MG. However, this goal should be achieved with the minimum cost. Hence, tuning these parameters has been modeled as a multi-objective optimization problem which considers both stability and economic aspects. Considering the fact that usual multi-objective optimization algorithms, like non-dominated sorting genetic algorithm II (NSGA-II), would not show a good performance in solving optimization problems with more than three objectives [16], a recently developed many-objective knee point driven evolutionary algorithm (KnEA) is implemented for solving this problem. Finally, to select one of the Pareto optimal solutions obtained by KnEA as the final solution, a strategy based on the minimum sum of the normalized objectives is suggested. Also, a method for determining the characteristics of the ultracapacitor required for emulating the determined inertia is proposed.

The rest of this paper is organized as follows: in Section 2, the required equipment for increasing the inertia constant of the MG is studied. In Section 3, the process of tuning the parameters of MG for improving its frequency response is explained. The studied MG is introduced in Section 4. Then, in Section 5, by simulation studies carried out in Matlab/Simulink, the effectiveness of the proposed method is investigated. Finally, the conclusions of this research are presented in Section 6.

## 2. Increasing the inertia constant of MG

In this paper, the proper value of inertia constant together with frequency droop coefficient of DERs and load frequency controllers parameters are tuned to improve the frequency stability. To contribute to the inertial response, the power reference of inverter-based DERs should be altered as follows [17]:

$$P_{ref-new} = P_{ref-old} - 2H_{vir} \cdot \frac{df}{dt} \quad (1)$$

where $P_{ref-old}$, $P_{ref-new}$, $H_{vir}$ and $f$ are the reference power without inertia emulation (in pu), the reference power with inertia emula-

tion (in pu), the value of virtual inertia (in pu s/Hz) and operation frequency of the grid (in Hz), respectively.

The energy storages used for providing inertial power should be able to contribute to the inertia of the grid until the frequency reaches its critical value. Hence, the required energy for contributing to inertial response with an inertia constant of $H_{vir}$ is determined as:

$$E = \int_0^{t_{crit}} P_{inertia}\,dt = \int_0^{t_{crit}} -2H_{vir}\cdot\frac{df}{dt}\,dt = \int_{f_{init}}^{f_{crit}} -2H_{vir}\,df = 2H_{vir}\,(f_{init} - f_{crit}) \quad (2)$$

where $P_{inertia}$, $f_{init}$, $f_{crit}$ and $t_{crit}$ are the inertial power (in pu), the frequency before the disturbance (in Hz), the critical frequency (in Hz) and the time it takes the frequency to reach $f_{crit}$ (in s), respectively. It can be assumed that the frequency of the grid before the disturbance equals to the nominal value ($f_n$).

In case of using energy storages such as UC for emulating the inertial response, their capacity and maximum power should be designed. The energy stored in UC depends on its capacitance and nominal voltage. As the UC cannot be fully discharged and its stored energy can be extracted until the voltage reaches a specified value [18], the energy available from UC for inertial response (in pu s) is:

$$E_{avail} = \frac{C}{2}\left(V_{init}^2 - V_{min}^2\right)\frac{1}{P_{base}} \quad (3)$$

where $C$, $V_{init}$, $V_{min}$ and $P_{base}$ are the capacitance (in F), initial voltage (in V), minimum permissible voltage of UC (in V) and base power of the grid (in W). It can be assumed that the initial voltage of UC before the disturbance is equal to the nominal value ($V_n$). Based on Eqs. (2) and (3) the required capacitance of UC for emulating an inertia constant equal to $H_{vir}$ is:

$$C_{req} = 4H_{vir}\cdot\frac{(f_n - f_{crit})}{\left(V_n^2 - V_{min}^2\right)}.P_{base} \quad (4)$$

Hence, the nominal stored energy of UC (in pu s) will be:

$$E_n = \frac{1}{2}C_{req}V_n^2\frac{1}{P_{base}} = 2H_{vir}\cdot\frac{(f_n - f_{crit})}{\left(V_n^2 - V_{min}^2\right)}.V_n^2 \quad (5)$$

The nominal power of the UC (in pu) can be defined such that the UC is able to inject the required inertial power to grid in case of the worst contingency:

$$P_n = 2H_{vir}.\max\left|\frac{df}{dt}\right| \quad (6)$$

where $\max|\frac{df}{dt}|$ is the highest rate of frequency decay (in Hz/s) which happens immediately after the occurrence of the worst contingency.

In Section 3, a method for determining the required inertia constant together with some tunable parameters of MG is proposed. Subtracting the inherent inertia constant of MG from the minimum required value of inertia constant, the value of inertia that should be virtually emulated is calculated.

## 3. Improving frequency response and stability of MGs by tuning H, R and load frequency controllers

Increasing $H$ and $1/R$ would decrease the maximum frequency deviation. $1/R$ is referred to as primary frequency control gain. On the other hand, while increasing $H$ decreases the amplitude of frequency oscillations, increasing $1/R$ above a specific value would increase the amplitude of these oscillations. Also, fine tuning the load frequency controllers, which are responsible for bringing the frequency deviation back to zero, improves the frequency response of MG. Hence, $H$ and $R$ would be tuned together with load frequency controllers to result in a smooth frequency response that does not violate the specified limits. For this purpose, determining the proper criteria and using an effective method for tuning the parameters, such that these criteria are met, is of great importance.

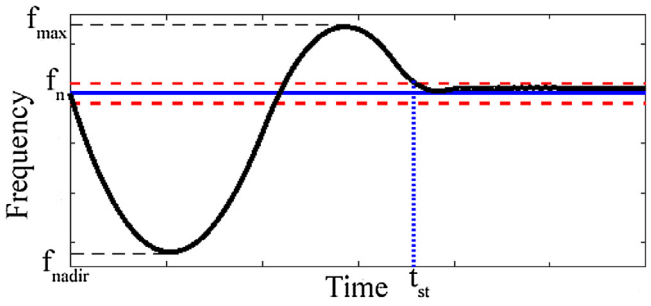


**Fig. 1.** Frequency of the MG after a power deficit.

### 3.1. Objective functions and problem formulation

The typical behavior of frequency of an MG after a power deficit is shown in Fig. 1. As can be seen in this figure, frequency undershoot ($f_{nadir}$), frequency overshoot ($f_{max}$) and the time after which frequency deviation from the nominal value returns to the desired region ($t_{st}$) are important characteristics of frequency response that should be minimized. These goals would be achieved by determining the proper values of $R$ and $H$ together with the parameters of PID load frequency controllers ($K_P$, $K_I$ and $K_D$). It is important to tune these parameters such that the goals are achieved with the minimum cost. In the following, the objective functions that should be optimized for fine tuning the parameters of an MG are discussed.

The purpose of the frequency control in MG, in case of a power imbalance, is to minimize the maximum frequency deviation while bringing the frequency back to the desirable region as soon as possible. It is also important to have a zero steady state frequency deviation. The first goal would be achieved by minimizing $Obj_1$ and $Obj_2$ which are defined as a function of frequency undershoot and overshoot in Fig. 1, respectively.

$$Obj_1 = f_n - f_{nadir} \quad (7)$$

$$Obj_2 = f_{max} - f_n \quad (8)$$

where $f_n$ is the nominal frequency.

The second goal would be achieved by considering the settling time, denoted by $t_{st}$ in Fig. 1, as the third objective:

$$Obj_3 = t_{st} \quad (9)$$

where $t_{st}$ is the time after which the frequency deviation will remain smaller than 2% of the maximum deviation for the studied disturbance.

Although (9) minimizes the settling time, it cannot guarantee the zero steady state frequency error; i.e. the frequency might have low amplitude oscillations around the nominal value. Zero steady state frequency deviation is achieved by minimizing the integral of time multiplied by absolute error (ITAE):

$$Obj_4 = \int_0^{t_{sim}} t \times |\Delta f(t)|\,dt \quad (10)$$

where $t$ is time and $\Delta f(t)$ is deviation of the frequency from the nominal value ($\Delta f(t) = f(t) - f_n$) and $t_{sim}$ is the simulation time. This objective function also would result in a reduction in frequency oscillations. Furthermore, it would affect the settling time. However, since some other conflicting factors such as the maximum frequency deviation are considered in Eq. (10), to minimize the settling time, it is necessary to consider Eq. (9) as one of the objective functions.

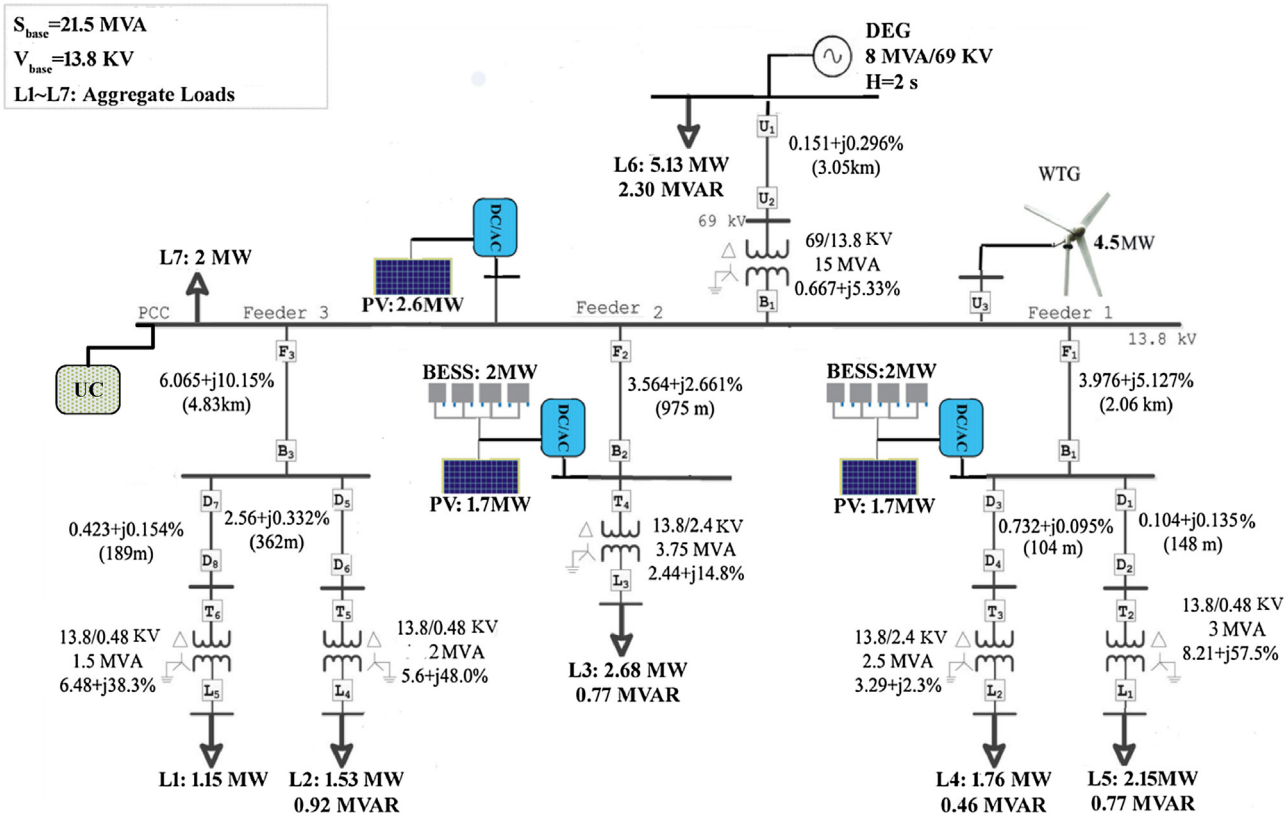


**Fig. 2.** Studied microgrid.

The above objective functions are minimized by optimal tuning the load frequency controllers' parameters, frequency droop coefficient of DERs and inertia constant of MG. However, to increase the inertia constant of MG, energy storages are required. Higher inertia constant will result in a higher cost of energy storages. Hence, minimizing $H$ would be considered as the next objective of this problem:

$$Obj_5 = H \tag{11}$$

where $H$ is the sum of the equivalent inertia constant of the online synchronous generators ($H_{eq}$) and the inertia constant which is going to be virtually emulated ($H_{vir}$); i.e $H = H_{eq} + H_{vir}$.

To tune load frequency controllers parameters, frequency droop coefficient of DERs and the equivalent inertia constant of the MG, the optimization problem would be formulated as follows:

$$Minimize\ (obj_1(x), obj_2(x), \ldots obj_5(x))$$

$$x = (K_{P\_1}, K_{I\_1}, K_{D\_1}, \ldots, K_{P\_n}, K_{I\_n}, K_{D\_n}, R_1, \ldots, R_n, H) \tag{12}$$

$$S.t.\ f_{nadir} > f_{min}$$

$$x^{low} \le x \le x^{up}$$

The constraint prevents the frequency from falling below the minimum desirable value ($f_{min}$). $x$ represents the decision variables vector, $n$ is the number of DERs that participate in primary frequency control and load frequency control. Also, $x^{up}$ and $x^{low}$ are the upper and lower limit vectors for the decision variables.

### 3.2. Solving the optimization problem

In Section 3.1, several objectives have been introduced to be minimized for improving the frequency response and stability of the MG with the minimum cost. Because of the conflicting nature of the objectives, for the problems of this type, generally there is a set of trade-off solutions known as Pareto optimal solutions. This type of problems can be solved by means of multi-objective evolutionary algorithms to obtain a set of Pareto optimal solutions.

However, due to the fact that the number of objectives is higher than three, ordinary evolutionary algorithms would not show a good performance in solving this problem and many-objective optimization algorithms should be used to solve it [16]. Knee point driven evolutionary algorithm (KnEA) is a many-objective optimization algorithm which has been newly proposed in Ref. [16]. The superiority of this algorithm in solving many-objective optimization problems over some other multi-objective algorithms has been proved in Ref. [16]. Hence, KnEA has been implemented for solving the many-objective optimization problem defined in this paper.

#### 3.2.1. Solving process

Principally, KnEA is an elitist Pareto-based multi-objective evolutionary algorithm. The main difference between KnEA and other Pareto-based multi-objective evolutionary algorithms like NSGA-II is using knee points as a secondary selection criterion besides dominance relationship. Adding this criterion to the selection process has improved the performance of KnEA in solving many-objective optimization problems. In Pareto front, a knee point refers to the solution in which a small improvement in one objective of such a solution results in a severe degradation in at least one of the other objectives.

The main steps of KnEA for solving the many-objective problem of tuning of MG parameters are presented below. More details on KnEA would be found in Ref. [16].

1. Initialization: In this step the input parameters, including the population size ($N$), number of iterations, the ratio of knee points and the upper/lower limits of decision variables are entered. Then, the initial sets of MG parameters $x = (K_{P\_1}, K_{I\_1}, K_{D\_1}, ..., K_{P\_n}, K_{I\_n}, K_{D\_n}, R_1, ..., R_n, H)$ are randomly generated.
2. Calculating the values of the objective functions: The dynamic MG model simulated in Matlab/Simulink is run and the objective functions in case of the specified disturbances are calculated for each member of MG parameters set. For the members that resulted in violation from the constraint, as a penalty mechanism, the value of the objectives are multiplied by 1000.
3. Binary tournament selection: In the binary tournament selection, three tournament metrics including the dominance relationship, weighted distance measure, and the knee point criterion are implemented, to choose individuals from the parent sets of MG parameters for generating $N$ offspring sets based on a variation method. In fact, in the binary tournament mating selection, two solutions are selected randomly from the parent population set. If one of the solutions is dominated by the other one, then the later solution is selected. If none of solutions can dominate the other one, it will be checked whether they are knee points. If only one of these two solutions can be considered as a knee point, then the knee point is selected from the parent set. Otherwise, a weighted distance will be used for comparing the two solutions and the solution which has a larger weighted distance will win the tournament. If the weighted distances of both solutions are the same, one of them will be selected randomly for reproduction.
4. Non-dominated sorting and identifying the knee points: Non-dominated sorting is used to form non-dominated fronts. Different methods have been proposed in literature for this purpose. In KnEA, due to its computational efficiency, the non-dominated sorting method proposed in Ref. [19], is employed. Then an adaptive strategy, which is thoroughly explained in Ref. [16], is taken to identify the knee points of non-dominated fronts.
5. Environmental selection: To select $N$ individuals as the parent sets of MG parameters of the next generation, environmental selection is performed. Before doing environmental selection, KnEA performs non-dominated sorting as explained in Ref. [19] to form $N_F$ non-dominated fronts. Then, it starts choosing the non-dominated solutions from the first non-dominated front ($F_1$). When the number of solutions in $F_1$ is higher than the population size $N$, the knee points located in $F_1$ are chosen as parents for the next population. If the number of knee points ($N_{P1}$) is also larger than $N$, then $N$ knee points with a larger distance from the hyperplane are chosen. Otherwise, $N_{P1}$ knee points together with $(N - N_{P1})$ other solutions in $F_1$ with a larger distance from the hyperplane of $F_1$ are selected. When the number of solutions in $F_1$ is smaller than $N$, KnEA selects $(N - |F_1|)$ parent solutions from the second non-dominated front based on a procedure similar to what explained for $F_1$. This process is repeated until $N$ parent population for the next generation is found.

The above procedure repeats until the maximum number of iterations is reached. In the end, the algorithm produces a number of Pareto optimal solutions among which one has to be selected as the final solution. The procedure of selecting one of the Pareto optimal solutions as the final solution is explained in Section 3.2.2.

*3.2.2. Selecting the final solution*

When the stop criterion is met, the optimization algorithm will give us a number of Pareto optimal solutions among which one has to be chosen as the final solution. Here, a measure based on the sum of the normalized objectives has been proposed to select one of the $N$ Pareto optimal solutions as the final solution:

$$d^l = \sum_{i=1}^{m} \left( \frac{Obj_l i Ideal\_Obj_i}{} \right) \tag{13}$$

where the $Obj_{li}$ is the $i$th objective of the $l$th Pareto optimal solution, $m$ is the number of objectives and $Ideal\_Obj_i$ is the $i$th element of the ideal objective vector which is defined as follows:

$$Ideal\_Obj = \left[ \min_{l=1\to N} obj_1^l, \min_{l=1\to N} obj_2^l, \ldots, \min_{l=1\to N} obj_m^l \right]$$

The $i$th element of this vector equals to the minimum non-zero value of the $i$th objective among all the obtained Pareto optimal solutions.

The Pareto optimal solutions would be ranked based on the $d$ calculated for each solution and if the solution with the minimum $d$ is not satisfactory for the decision maker, the other solutions can be considered according to their rank.

## 4. Studied MG

### 4.1. Configuration of the studied microgrid

To illustrate the effectiveness of the proposed method for improving the frequency stability of MGs, a microgrid with various DERs including wind turbine generator (WTG), photovoltaic (PV), diesel engine generator (DEG) and battery energy storage system (BESS) has been studied. In this system, PV and WTG are controlled to inject the maximum power to the grid and are not dispatchable. But, DEG and BESS participate in frequency control.

The studied MG which is shown in Fig. 2 is a modified IEEE standard distribution system [20,21]. An eighth order model is used for synchronous generator. Diesel engine and governor are represented by the following transfer function [22]:

$$G_{DEG}(s) = \frac{1}{(1 + sT_g)(1 + sT_t)} \tag{14}$$

where $T_g$ and $T_t$ are governor and turbine time constants, respectively.

The model used for BESS is [22]:

$$G_{BESS}(s) = \frac{K_{BESS}}{(1 + sT_{BESS})} \tag{15}$$

UC which is implemented for inertia emulation is modeled by the following transfer function [8]:

$$G_{UC}(s) = \frac{1}{(1 + sT_{UC})} \tag{16}$$

Considering the fact that the rate of change of output power of each DER is limited and this would highly affect their frequency response, the ramp up and ramp down rate of the output power of these DERs has been considered as [23]:

$$\dot{P}_{BESS} < 20\%/\text{s}, \quad \dot{P}_{DEG} < 40\%/\text{min}$$

The effect of frequency and voltage dependency of loads on the active and reactive powers is modeled as follows [24]:

$$\begin{aligned} P_L &= P_{L0}\left(\frac{V}{V_0}\right)^{\alpha}(1 + K_{pf}\Delta f) \\ Q_L &= Q_{L0}\left(\frac{V}{V_0}\right)^{b}(1 + K_{qf}\Delta \text{f}) \end{aligned} \tag{17}$$

where $P_L$, $P_{L0}$, $V$, $V_0$, $a$, and $K_{pf}$ are current load active power, initial active power of the load, load voltage, initial voltage of load, voltage dependency coefficient of active power and frequency dependency coefficient of active power, respectively. Also, $Q_L$, $Q_{L0}$, $b$, and $K_{qf}$

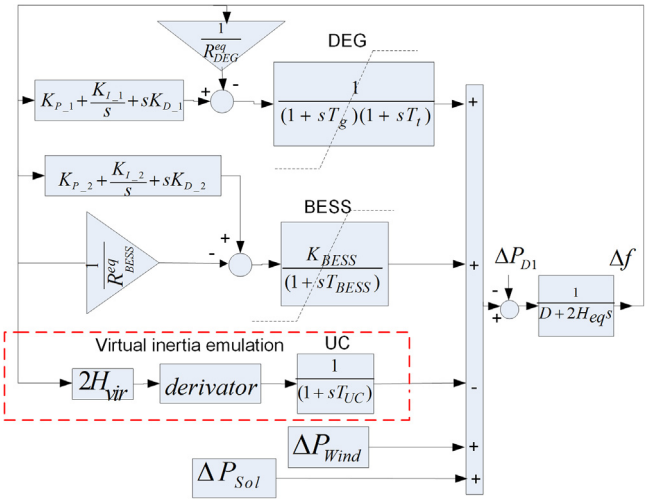


**Fig. 3.** Frequency response model of the studied MG.

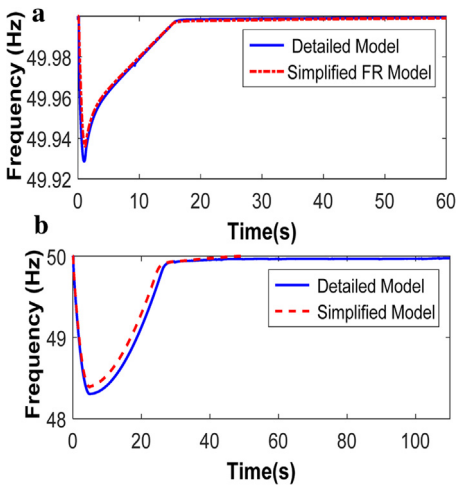


**Fig. 4.** Comparison between the response of the detailed model and the simplified frequency response model: (a) in case of a 0.86 MW power deficit and (b) in case of a 4.5 MW power deficit.

are current load reactive power, initial reactive power of the load, voltage dependency coefficient of reactive power and frequency dependency coefficient of reactive power, respectively.

The value of parameters of DERs and loads are taken from Refs. [8,20,22,24] and given in Appendix A.

### 4.2. Frequency response model

To decrease the computational cost of solving the optimization problem, it is desirable to simplify the model used for frequency response studies. In isolated power systems, frequency dynamics are mainly affected by rotor and governor-turbine system dynamics. Exciter and generator transients are much faster and can be neglected [8]. Hence, the frequency response model shown in Fig. 3 is accurate enough for investigating the frequency response of MGs in case of power imbalances [8,22]. In this model, $H_{eq}$ and $D$ are the equivalent inertia constant of the synchronous generators and load damping factor. Load damping factor models the dependency of loads power in frequency. $R^{eq}{}_{BESS}$ and $R^{eq}{}_{DEG}$ are the equivalent frequency droop coefficient of BESS and the equivalent frequency droop coefficient of DEGs, respectively. $H_{eq}$ (in pu s/Hz) can be calculated as follows [24]:

$$H_{eq} = \frac{\sum_{i=1}^{n} H_i S_i}{f_n . S_{base}} \tag{18}$$

where $H_i$, $S_i$, $S_{base}$ and $n$ are the inertia constant of the $i$th synchronous generator (in s), the nominal capacity of the $i$th synchronous generator (in MVA), the base power of MG (in MVA) and the number of the synchronous generators, respectively.

To calculate load damping factor from the detailed model of MG, it is assumed that DERs do not contribute to the frequency response. If a power deficit with the magnitude of $P_D$ (in pu) occurs in such a case, by measuring the steady state frequency deviation ($\Delta f_{ss}$ in Hz), load damping factor (in pu/Hz) would be calculated as follows:

$$D = \frac{P_D}{\Delta f_{ss}} \tag{19}$$

Also, for online estimation of the equivalent inertia constant of power systems and load damping factor, some methods have been proposed in Refs. [25,26].

Fig. 4 which compares the frequency obtained using the detailed model of MG and the simplified frequency response model depicted in Fig. 3, shows that the frequency response model has a good accuracy in case of both small and large disturbances. The optimal parameters presented in the second row of Table 2, have been used in these simulations.

Due to the fact that the frequency response model has a good accuracy and calculation of frequency using this model considerably reduces the computational cost, this model has been used for the optimization process. Also, the simulation results presented in the next section are obtained using the frequency response model.

The upper and lower limits of the decision variables of the optimization problem are considered as: $0.0149 < H < 0.2$ pu s/Hz, $0 < 1/R_1 < 5$ pu/Hz, $0 < 1/R_2 < 5$ pu/Hz, $-5 < K_{P\_1} < 5$, $-5 < K_{I\_1} < 5$, $-5 < K_{D\_1} < 5$, $-5 < K_{P\_2} < 5$, $-5 < K_{I\_2} < 5$, $-5 < K_{D\_2} < 5$.

## 5. Results and analysis

In this section, the necessity of increasing the inertia constant of a low inertia MG for achieving an acceptable frequency response has been investigated and different strategies for tuning the parameters of MG have been compared.

As the emulated inertia constant is dependent on the capacity of the installed UC, increasing it will require an increase in the capacity of UC. Hence, a value for the emulated inertia constant should be determined that is enough for keeping the frequency stability of the MG, in case of the worst contingency, in all operating conditions. The worst operating condition from the frequency stability point of view is when the system has the minimum load, which results in the lowest load damping factor, and the renewables produce their maximum power, which results in the lowest inertia constant. Such an operating condition for the studied MG, including loads power and renewables generation, is shown in Fig. 2. The inertia constant, frequency droop coefficient of DERs and load frequency controllers parameters are tuned such that the frequency is kept above $f_{min}$ if the worst contingency happens when the system has the lowest value of $H_{eq}$ and $D$. The tuned parameters would be fixed for all the operating conditions of the MG.

While lower values of $R$ result in lower frequency deviations in case of small disturbances, they might result in oscillatory frequency response in case of large disturbances. Hence, the optimization problem is simultaneously solved for a small and large disturbance to guarantee the acceptable operation of MG in case of both small and large disturbances. In this section, the worst contingency which is in the scope of load frequency control (a 4.5 MW power deficit), is considered as the large contingency and the minimum allowed frequency of the MG before activating the

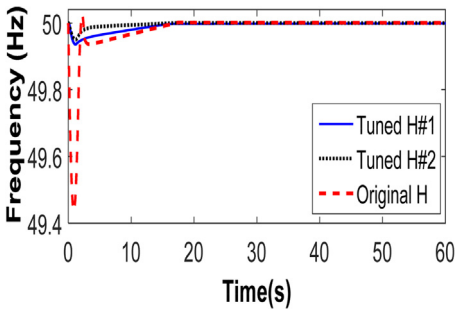


**Fig. 5.** Frequency of the MG in case of a 0.86 MW power deficit.

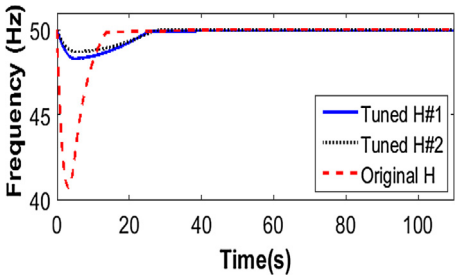


**Fig. 6.** Frequency of the MG in case of a 4.5 MW power deficit.

underfrequency load shedding relays (48 Hz) is considered as $f_{min}$ for this case. On the other hand, a 0.86 MW disturbance is considered as the small disturbance for which the problem is solved. The value of $f_{min}$ for this case is considered to be 49.5 Hz. $t_{sim}$ used for optimization equals 1000 s.

### 5.1. Comparison between the performance of different strategies used for tuning the parameters

To investigate the necessity of tuning $H$, firstly, only load frequency controllers and frequency droop coefficient of DERs are tuned (the inertia constant has not been tuned); this strategy is called Original H. Then, $H$ has been tuned together with controllers and frequency droop coefficient of DERs and this strategy is called Tuned H#1. Finally, to show the effect of considering $H$ as one of the objectives, $H$ has been considered as one of the decision variables to be tuned together with controllers and frequency droop coefficient of DERs but $Obj_5$ is omitted; this strategy is called Tuned H#2. After the termination of optimization process, MO algorithm achieves a set of Pareto optimal solutions. A number of the Pareto optimal solutions of Tuned H#1 strategy are given in Table 1. The objectives with superscript 1 and 2 are related to the large and small disturbance, respectively. $Obj_5$ is the inertia constant of the MG and is the same for both disturbances. There are solutions with higher inertia which result in lower frequency deviation. However, these solutions will impose a higher cost of energy storages.

Here, the Pareto optimal solutions are ranked according to their respective $d$ calculated using Eq. (13) and then one is chosen as the final solution based on its $d$ and the decision maker preference. As can be seen from Table 1, solution number 7 has the lowest $d$ and it has been selected as the final solution. The parameters of the MG tuned by different strategies are given in Table 2. Fig. 5 shows that in case of the small disturbance (0.86 MW), Original H could preserve frequency stability. However, the frequency deviation is higher than Tuned H#1 and Tuned H#2 strategies. As Fig. 6 shows, using the parameters tuned by Original H strategy, the frequency violates the minimum permissible limit in case of the worst contingency which is in the scope of load frequency controllers. In fact, this figure shows that when $H$ is not tuned, the optimization

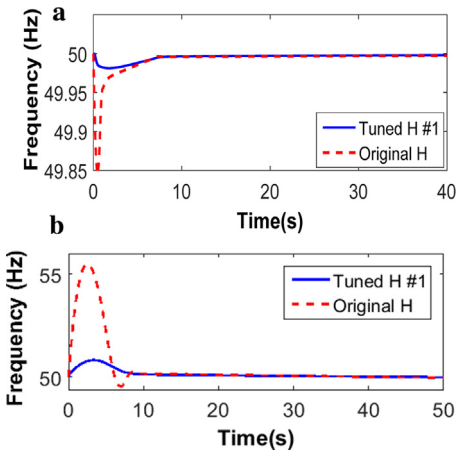


**Fig. 7.** Frequency of the MG: (a) in case of 0.43 MW power deficit and (b) in case of a 3.22 MW power surplus.

algorithm could not achieve any solution that does not violate the minimum permissible limit. This certifies the necessity of tuning $H$ for achieving a solution which does not violate the optimization constraint.

Having determined the value of virtual inertia, the required power and energy specification of UC is determined based on the method explained in Section 2. To emulate the inertia constant determined by Tuned H#1 strategy, a UC with nominal power of 5.87 MW and stored energy of 23.92 MW.s is required. However, if the parameters determined by Tuned H#2 strategy are going to be used, a UC with nominal power of 6.01 MW and stored energy of 31.83 MW.s will be required. From Figs. 5 and 6 it can be found that using the parameters tuned by the Tuned H#1 and Tuned H#2 strategies, the frequency of MG is maintained within the permissible limits in case of both large and small disturbances. Using the parameters obtained by Tuned H#2 strategy, MG experiences a smaller frequency deviation in case of both large and small disturbances. However, Tuned H#2 strategy has led to a UC with a higher capacity. Considering a 200 €/kW cost of installation for power and a 10 k€/kWh cost of installation for energy [8], the UC installation cost will be 1240 k€ and 1290 k€ for the Tuned H#1 and Tuned H#2 strategies, respectively.

It is also worth mentioning that a computer with a 24 GB RAM and a 2.93 GHz CPU with 24 cores has been used for solving the optimization problems. The optimization process elapsed 832, 965 and 1385 s for the Tuned H#1, Tuned H#2 and Original H methods, respectively.

### 5.2. Performance of Tuned H#1 and Original H strategies for different power imbalances

In the studied MG, load frequency controllers should keep the frequency above 48 Hz in case of power deficits less than 4.5 MW and load shedding might be triggered for the larger disturbances to keep the minimum frequency above 47 Hz [8,27]. Here, the underfrequency load shedding method proposed in Ref. [21], has been implemented. However, according to the requirements of the studied MG, the thresholds for activating the load shedding steps have been altered to the following values: 48, 47.8, 47.6 and 47.4 Hz. In this section, some case studies are carried out to investigate the frequency response of MG with the designed parameters.

#### 5.2.1. Case I: a 0.43 MW step increase in demand

Fig. 7(a) shows the frequency response of the system in case of a 0.43 MW step increase in demand. It is clear that both of the Tuned H#1 and Original H strategies could maintain the frequency within

**Table 1**
The value of objectives for a number of pareto optimal solutions obtained by KnEA (superscript 1 and 2 refer to the large and small disturbance, respectively).

| | $Obj_1{}^1$ | $Obj_1{}^2$ | $Obj_2{}^1$ | $Obj_2{}^2$ | $Obj_3{}^1$ | $Obj_3{}^2$ | $Obj_4{}^1$ | $Obj_4{}^2$ | $Obj_5$ | $d$ |
|---|---|---|---|---|---|---|---|---|---|---|
| 1 | 1.36 | 0.05 | 0.008 | 0.00 | 37.7 | 20.4 | 589 | 2.8428 | 0.1888 | 32 |
| 2 | 1.51 | 0.06 | 0.011 | 0.00 | 35.8 | 16.0 | 706 | 3.5431 | 0.1688 | 50 |
| 3 | 1.68 | 0.06 | 0.014 | 0.000 | 37.1 | 16.9 | 766 | 4.0333 | 0.1499 | 51 |
| 4 | 1.74 | 0.07 | 0.007 | 0.003 | 36.9 | 35.1 | 599 | 4.7951 | 0.1441 | 73 |
| 5 | 1.90 | 0.07 | 0.022 | 0.000 | 25.3 | 15.1 | 1701 | 1.6329 | 0.1303 | 62 |
| 6 | 1.38 | 0.05 | 0.000 | 0.026 | 41.3 | 44.5 | 506 | 10.61 | 0.1858 | 290 |
| 7 | 1.63 | 0.06 | 0.000 | 0.00 | 39.6 | 43.7 | 602 | 8.8980 | 0.1540 | 28 |
| 8 | 1.61 | 0.06 | 0.0589 | 0.005 | 97.1 | 40 | 2719 | 3.040 | 0.1566 | 207 |
| Ideal Obj | 1.34 | 0.05 | 0.0005 | 0.0001 | 25.3 | 9.4 | 390 | 0.5120 | 0.1272 | – |

**Table 2**
Parameters of the studied MG tuned based on different strategies.

| | $\frac{1}{R^{eq}_{DEG}}\ (pu/Hz)$ | $\frac{1}{R^{eq}_{BESS}}\ (pu/Hz)$ | $H\ (pus/Hz)$ | $K_{P_1}$ | $K_{I_1}$ | $K_{D_1}$ | $K_{P_2}$ | $K_{I_2}$ | $K_{D_2}$ |
|---|---|---|---|---|---|---|---|---|---|
| Tuned H#1 | 0.5682 | 0.7058 | 0.1540 | −2.0719 | −0.0721 | −1.7581 | −0.1249 | −0.0030 | −0.5424 |
| Tuned H#2 | 1 | 0.9924 | 0.2000 | −0.1530 | −0.2496 | −0.7481 | −1.9500 | −0.0039 | −1.9280 |
| Original H | 1 | 0.9168 | – | −1.3220 | −0.0362 | −0.7673 | 0.3896 | −0.0017 | −0.1215 |

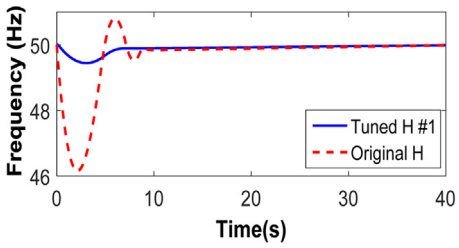


**Fig. 8.** Frequency of the MG in case of the largest PV unit outage.

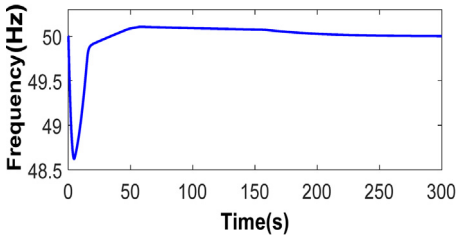


**Fig. 9.** Frequency of the MG in case of a 4.5 MW power deficit when the load has increased by 30%.

the allowed limits. However, using Tuned H#1, MG will experience a smaller frequency deviation.

*5.2.2. Case II: a 3.2 MW step decrease in demand*

It can be found from Fig. 7(b) that as a result of a 3.2 MW step increase in the demand of MG, the performance of Original H strategy has been significantly deteriorated and the frequency goes considerably above the permissible limit. However, using Tuned H#1 strategy the frequency stability of MG in case of this power surplus has been preserved.

*5.2.3. Case III: largest PV unit outage*

The output power of PV units might change as a result of changes in the temperature and sun irradiance [28]. Fig. 8 shows the frequency response of the studied MG when the power generated by the largest PV unit falls from the maximum value (2.6 MW) to zero. Using the parameters obtained by Original H strategy, frequency goes considerably below 48 Hz and underfrequency load shedding should be carried out in this case to prevent the frequency from falling below the minimum acceptable value. On the other hand, using the parameters tuned by the Tuned H#1 strategy, the frequency is maintained within the permissible limits and underfrequency load shedding is not required.

*5.3. Load shedding*

In this section, the frequency response of the studied MG with the parameters tuned using the proposed Tuned H#1 strategy is investigated, for different contingencies which require load shedding, and compared with the Original H strategy.

Table 3 demonstrates that in case of large power deficits, using the parameters obtained by both strategies, the load shedding scheme was successful in stopping the frequency decline. However, using the parameters tuned by the Tuned H#1 strategy, load shedding is avoided in many cases and in the other cases the amount of load shedding is considerably lower than when the parameters tuned by Original H strategy are used. In this way, a better quality of service would be provided for the customers and their satisfaction level is increased.

*5.4. Robustness of MG using the parameters tuned with the proposed method*

In any power system, load changes with the time and this would change the operating point of the system. But, as the emulated inertia constant depends on the installed capacity of the UC, it cannot be increased to the values higher than the designed value. Fig. 9 shows that the parameters designed for the minimum load conditions, are able to maintain the frequency stability in case of the worst contingency (a 4.5 MW power deficit) when the load of system has increased by 30%. To supply the load in this case, another 8 MVA DEG has been connected to the 69 KV bus of the system. It should be mentioned that for a better operation of the MG, the parameters of the system except $H$ would be retuned if the operation conditions changed considerably.

Also, it is possible that there is an inaccuracy in the parameters estimated for modeling the system. Even the parameters of the system might change by time [29]. Hence, it is important to investigate the performance of the MG in case of parameters variations. Fig. 10 shows that, using Tuned H#1 strategy, MG has an acceptable frequency response in case of a 4.5 MW power deficit when the total $H$ and $D$ of the MG are 10% higher/lower than the nominal values. Furthermore, as shown in Fig. 11, 10% decrease/increase in the time constants of DERs ($T_{BESS}$, $T_g$, $T_t$ and $T_{UC}$) does not have a considerable effect on the frequency response of MG.

**Table 3**
Performance of the MG in case of sever power deficits.

| $P_d$(pu) | | 0.10 | 0.15 | 0.20 | 0.25 | 0.30 |
|---|---|---|---|---|---|---|
| Original H strategy | $P_{shed}$ (pu) | 0.0198 | 0.0809 | 0.1490 | 0.2053 | 0.2593 |
| | $f_{nadir}$ (Hz) | 47.51 | 47.41 | 47.40 | 47.39 | 47.39 |
| Tuned H#1 strategy | $P_{shed}$ (pu) | 0 | 0 | 0 | 0.0152 | 0.0829 |
| | $f_{nadir}$ (Hz) | 49.61 | 49.14 | 48.48 | 47.40 | 47.54 |

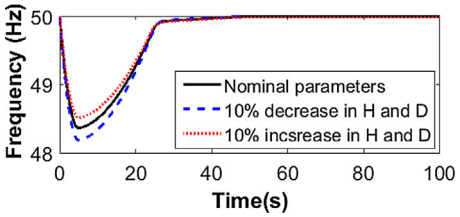


**Fig. 10.** The effect of change in *H* and *D* on the frequency response of MG in case of a 4.5 MW power deficit.

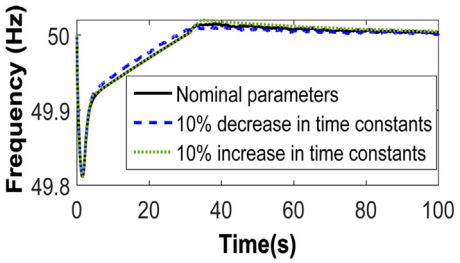


**Fig. 11.** The effect of change in the time constants of DERs on the frequency response of MG in case of a 1.5 MW power deficit.

## 6. Conclusion

In this paper, improving the frequency stability of low inertia MGs was investigated. It has been shown that fine-tuning the load frequency controllers' parameters and frequency droop coefficient of DERs, could not solely guarantee the frequency stability of low inertia MGs. Hence, tuning the inertia constant together with load frequency controllers' parameters and frequency droop coefficient of DERs has been proposed in this paper for improving the frequency stability of low inertia MGs. In fact, tuning these parameters has been modeled as a multi-objective optimization problem which considers both technical and economic concerns. Because the number of objectives is higher than three, a many-objective optimization algorithm has been implemented for solving this problem. Additional finding from the studies carried out in the paper are:

1. KnEA has a good performance in solving the optimization problem determined in this paper.
2. Tuning the parameters of the MG with the proposed MO method has highly improved its frequency response.
3. Comparing the proposed Tuned H#1 strategy with the Original H method certifies the necessity of determining the proper value of inertia constant in low inertia MGs.
4. Using the parameters tuned by the proposed method, MG has a good performance in case of changes in the operating conditions of MG and its parameters.

## Appendix A.

The parameters of the studied MG:

$K_{BESS} = 1,\ D = 0.012\,\text{pu/Hz},\ H = 0.0149\,\text{pu s/Hz},\ T_{BESS} = 0.1\,\text{s},$

$T_g = 0.08\,\text{s},\ T_t = 0.4\,\text{s},\ T_{UC} = 0.2\,\text{s}, P_{base} = 21.5\,\text{MW},\ K_{pf} = 0.012\,\text{pu/Hz},\ K_{qf} = 0.010\,\text{pu/Hz},\ a = 1\ b = 2.$

## References

[1] F.M. Uriarte, C. Smith, S.V. Broekhoven, R.E. Hebner, Microgrid ramp rates and the inertial stability margin, IEEE Trans. Power Syst. 30 (November (6)) (2015) 3209–3216.
[2] N. Mendis, K.M. Muttaqi, S. Perera, Management of battery-supercapacitor hybrid energy storage and synchronous condenser for isolated operation of PMSG based variable-speed wind turbine generating systems, IEEE Trans. Smart Grid 5 (March (2)) (2014) 944–953.
[3] Nahid-Al-Masood, R. Yan, T.K. Saha, N. Modi, Frequency response and its enhancement using synchronous condensers in presence of high wind penetration, in: IEEE Power & Energy Society General Meeting, Denver, CO, 2015, pp. 1–5.
[4] S. D'Arco, Jon Are Suul, O.B. Fosso, A Virtual Synchronous Machine implementation for distributed control of power converters in Smart Grids, Electr. Power Syst. Res. 122 (May) (2015) 180–197.
[5] T. Shintai, Y. Miura, T. Ise, Oscillation damping of a distributed generator using a virtual synchronous generator, IEEE Trans. Power Deliv. 29 (April (2)) (2014) 668–676.
[6] M.F.M. Arani, E.F. El-Saadany, Implementing virtual inertia in DFIG-based wind power generation, IEEE Trans. Power Syst. 28 (May (2)) (2013) 1373–1384.
[7] E. Rakhshani, D. Remon, A. Mir Cantarellas, P. Rodriguez, Analysis of derivative control based virtual inertia in multi-area high-voltage direct current interconnected power systems, IET Gener. Transm. Distrib. 10 (May (6)) (2016) 1458–1469.
[8] L. Sigrist, I. Egido, E. Lobato Miguélez, L. Rouco, Sizing and controller setting of ultracapacitors for frequency stability enhancement of small isolated power systems, IEEE Trans. Power Syst. 30 (July (4)) (2015) 2130–2138.
[9] A.M. Ersdal, L. Imsland, K. Uhlen, Model predictive load-frequency control, IEEE Trans. Power Syst. 31 (January (1)) (2016) 777–785.
[10] S. Mishra, G. Mallesham, A.N. Jha, Design of controller and communication for frequency regulation of a smart microgrid, IET Renew. Power Gener. 6 (July (4)) (2012) 248–258.
[11] Z.A. Obaid, L.M. Cipcigan, Ma. T. Muhssin, Fuzzy hierarchical approach-based optimal frequency control in the Great Britain power system, Electr. Power Syst. Res. 141 (December) (2016) 529–537.
[12] M.H. Khooban, T. Niknam, F. Blaabjerg, T.v Dragičević, A new load frequency control strategy for micro-grids with considering electrical vehicles, Electr. Power Syst. Res. 143 (February) (2017) 585–598.
[13] S.A. Taher, M. Hajiakbari Fini, S. Falahati Aliabadi, Fractional order PID controller design for LFC in electric power systems using imperialist competitive algorithm, Ain Shams Eng. J. 5 (March (1)) (2014) 121–135.
[14] A. Ketabi, M. Hajiakbari Fini, An adaptive set-point modulation technique to enhance the performance of load frequency controllers in a multi-area power system, J. Electr. Syst. Inf. Technol. 2 (December (3)) (2015) 391–405.
[15] J. Nanda, S. Mishra, L.C. Saikia, Maiden application of bacterial foraging based optimization technique in multiarea automatic generation control, IEEE Trans. Power Syst. 24 (May (2)) (2009) 602–609.
[16] X. Zhang, Y. Tian, Y. Jin, A knee point driven evolutionary algorithm for many-objective optimization, IEEE Trans. Evol. Comput. 19 (December (6)) (2015) 761–776.
[17] J. Morren, J. Pierik, S.W.H. de Haan, Inertial response of variable speed wind turbines, Electr. Power Syst. Res. 76 (July (11)) (2006) 980–987.
[18] Y. Brunet, Energy Storage, Wiley, Hoboken, NJ, USA, 2011.
[19] X. Zhang, Y. Tian, R. Cheng, Y. Jin, An efficient approach to nondominated sorting for evolutionary multiobjective optimization, IEEE Trans. Evol. Comput. 19 (April (2)) (2015) 201–213.
[20] S.A. Pourmousavi, M.H. Nehrir, Real-time central demand response for primary frequency regulation in microgrids, IEEE Trans. Smart Grid 3 (December (4)) (2012) 1988–1996.
[21] A. Ketabi, M. Hajiakbari Fini, An underfrequency load shedding scheme for hybrid and multiarea power systems, IEEE Trans. Smart Grid 6 (January (1)) (2015) 82–91.
[22] I. Pan, S. Das, Kriging based surrogate modeling for fractional order control of microgrids, IEEE Trans. Smart Grid 6 (January (1)) (2015) 36–44.

[23] V. Black, Cost and Performance Data for Power Generation Technologies, National Renewable Energy Laboratory, Golden, CO, 2012.
[24] P.S. Kundur, Power System Stability and Control, McGraw-Hill, New York, NY, USA, 1994.
[25] L.R. Chang-Chien, Y.S. Wu, J.S. Cheng, Online estimation of system parameters for artificial intelligence applications to load frequency control, IET Gener. Transm. Distrib. 5 (August (8)) (2011) 895–902.
[26] B. Polajžer, D. Dolinar, J. Ritonja, Estimation of area's frequency response characteristic during large frequency changes using local correlation, IEEE Trans. Power Syst. 31 (July (4)) (2016) 3160–3168.
[27] A. Ketabi, M. Hajiakbari Fini, Adaptive underfrequency load shedding using particle swarm optimization algorithm, J. Appl. Res. Technol. 15 (February (1)) (2017) 54–60.
[28] A. Ketabi, M. Hajiakbari Fini, An underfrequency load shedding scheme for islanded microgrids, Int. J. Electr. Power Energy Syst. 62 (November) (2014) 599–607.
[29] M. Hajiakbari Fini, G.R. Yousefi, H. Haes Alhelou, Comparative study on the performance of many-objective and single-objective optimisation algorithms in tuning load frequency controllers of multi-area power systems, IET Gener. Transm. Distrib. 10 (September (12)) (2016) 2915–2923.